

DYNAMICS OF NANO-SCALE ASSEMBLIES OF AMPHIPHILIC PEG-PDMS-PEG TRIBLOCK COPOLYMERS

Sudipta Gupta^{1*}, Rasangi M. Perera^{1*}, Christopher J. Van Leeuwen¹, Tianyu Li², Laura
Stingaciu³, Markus Bleuel^{4,5}, Kunlun Hong^{2,6} and Gerald J. Schneider^{1,7*}

¹*Department of Chemistry, Louisiana State University, Baton Rouge, LA 70803, USA*

²*Department of Materials Science and Engineering, University of Tennessee, Knoxville, TN
37996, USA*

³*Neutron Sciences Directorate, Oak Ridge National Laboratory, POB 2008, 1 Bethel Valley
Road, Oak Ridge, TN 37831, USA*

⁴*NIST Center for Neutron Research, National Institute of Standards and Technology,
Gaithersburg, MD 20899-8562, USA*

⁵*Department of Materials Science and Engineering, University of
Maryland, College Park, MD 20742-2115, USA*

⁶*Center for Nanophase Materials Sciences, Oak Ridge National Laboratory, Oak Ridge, TN
37831, USA*

⁷*Department of Physics & Astronomy, Louisiana State University, Baton Rouge, LA 70803,
USA*

Abstract

Micelles and vesicles are promising candidates in targeted drug/gene delivery, bioreactors, and templates for nanoparticle synthesis. We investigated the morphology and dynamics of PEG-PDMS-PEG triblock copolymer nano-scale assemblies regarding the membrane dynamics because the molecular dynamics of the membrane govern mechanical properties like the stability of a membrane. We studied the structure by cryogenic transmission electron microscopy, small-angle neutron scattering, and the dynamics by dynamic light scattering and neutron spin echo spectroscopy. We changed the length of the hydrophilic block to obtain micellar and vesicular systems. The vesicle has a membrane rigidity, $\kappa_{\eta} = 16 \pm 2 k_B T$, the same order of magnitude as the corresponding liposome value but one order of magnitude higher than polymeric interfaces in microemulsions. Hence, the height-height fluctuations of polymers in a polymersome seem much less than those measured for surfactants at an oil-water

interface. Therefore, the polymersome is substantially more stable. The value is very close to liposomes, indicating a similar stability.

1 Introduction

Amphiphilic triblock copolymers can self-assemble into different morphologies in aqueous solutions, including spherical micelles, rods, vesicles, disk-like, and other complex polymer aggregates such as giant compound micelles with an inverted core-shell structure surrounded by a hydrophilic surface.¹⁻⁸ Vesicles can further arrange from a simple spherical structure to elongated tubular or onion-like structures.^{8,9} Some of these nano-scale self-assembled structures have emerged as promising candidates as targeted drug/gene delivery agents, bioreactors, and templates for nanoparticle synthesis and to build cell-like structures and bioreactors.^{4, 10-18} Therefore, it is clear that the scope, application, and usage of self-assembled structures of polymers are vast fields, and studying the fundamental nature of the structure and dynamics of these assemblies is very important.

Studies on the self-assembled structures of these nano-scale assemblies are found excessively in the literature. Polymer chain length, hydrophilic to hydrophobic ratio between different blocks, polymer architecture, and solvent nature profoundly impact the structures' size and shape.¹⁹⁻²² Apart from those, external stimuli like salt concentration, temperature, and pH can influence the shape, size, and aggregation number transformations.²³⁻²⁶ The impact of these parameters has been demonstrated using a vast range of techniques, mainly but not limited to dynamic light scattering (DLS), microscopy, small-angle neutron scattering (SANS), and small-angle X-ray scattering (SAXS).^{13, 27-30} Often, these studies of morphology report shape deformation under external perturbations such as osmotic stress, temperature, and pH changes.^{24-26, 31-33}

The microscopic dynamics of these objects govern the macroscopic material response. For example, the use of micelles and polymersomes as drug/gene carriers may be related to the stability of these objects, which can be expressed in terms of the nanoscopic fluctuations.³⁴⁻³⁷ For biological membranes, changes in fluidity and composition of microdomains have been proven to regulate many critical physiological signaling pathways.³⁸ In other words, membranes exchange matter, energy, and information (signaling). Fluctuations on different length scales may lead to the formation of static or dynamic patches, so-called rafts, resulting in a heterogeneous state of matter in the membrane.^{39, 40} These phenomena can be applied to polymer vesicles and micelles in drug/gene delivery since their membranes are the first parts that would be in contact with

cellular/organelle membranes. Also, membrane thickness and rigidity affect the release rate of entrapped particles.⁴¹ Considering all these facts, it can be stressed that the study of molecular motions in the polymer self-assemblies is essential to give an insight into the changes in the membrane dynamics.

Thus far, studies of the polymer dynamics of membranes are rare. However, the experience from vesicular liposomes (vesicles resulting from phospholipid self-assemblies) shows the importance of bending and stretching moduli, lysis tension, and pore edge tension. Connecting the moduli and dynamics of membranes is highly relevant for drug delivery systems, where the membrane resistance to deformation may determine the behavior of a membrane. Hence, bending rigidity, area compressibility, or stretching elasticity modulus may be critical parameters to characterize the response of membranes, even with the complexity of the surrounding biological environment.⁴²

The key to understanding the dynamics of objects is morphology. To obtain objects of defined structures, we varied the amphiphilicity of the polymer. The self-assembled structure of a polymer can be explained by its hydrophilic-to-hydrophobic ratio.^{8, 43, 44} As a rule of thumb, if the hydrophilic mass fraction of a copolymer lies between 25-45%, it usually forms vesicles. Suppose the hydrophilic mass fraction of a copolymer lies between 45-55%. In that case, it favors the formation of cylindrical micelles, and at even higher hydrophilic mass fractions, the formation of spherical micelles is favored.^{44, 45} However, these ratios are not definitive features, and many exceptions can be found in the literature.⁸

Polymersomes with thicker and more rigid membranes than the lipid vesicle (liposome) membranes are expected to show higher bending rigidities, lysis tensions, and stretching elasticity values.⁴² It is essential to directly measure the membrane dynamics to verify existing models, extend our knowledge beyond the capabilities of current theory or simulations, and develop next-generation soft materials.

This study used two PEG-PDMS-PEG triblock copolymers with different hydrophilic weight fractions, which self-assembled into spherical micelles and vesicles. Both PEG and PDMS blocks of the triblock polymer find widespread applications. For example, PEG is one of the unique polymers specifically used in medical and biological applications.^{46, 47} Most of its biological applications include PEG-protein conjugates and PEG-modified small molecules for pharmaceutical applications, PEG tethers for biomolecule synthesis, PEG hydrogels for cell

encapsulation, drug delivery, and wound covering, and PEG-containing liposomes and micelles for drug delivery.^{48, 49} Its non-toxicity, non-immunogenicity, biocompatibility with blood and tissue, and solubility in a wide range of solvents offer various possibilities of utilization and explain the number of studies dealing with this polymer.^{50, 51} It is also one of the few FDA-approved polymers (Food and Drug Administration, USA).^{52, 53} Conversely, PDMS is widely used as an optically transparent, flexible, inert, nontoxic, non-flammable, biocompatible material. The low interacting methyl groups of the PDMS backbone cause bioinertness, which is why it has been routinely used as a biomedical implant material and for fundamental cellular studies.⁵⁴⁻⁵⁷

The bending rigidity of a membrane can be obtained by several techniques, including fluctuation spectroscopy, which is based on direct video microscopy observation of vesicles, methods based on mechanical deformation, molecular dynamics simulations, and Neutron Spin Echo (NSE) spectroscopy.^{35, 58-62} NSE techniques have been critical for studying liposomal or modified liposomal membranes.^{36, 62-64} The liposome results suggest that the NSE technique is beneficial for studying the dynamics of polymersomes.

This paper used DLS, SANS, and cryo-transmission electron microscopy (cryo-TEM) to characterize the static structure. NSE spectroscopy and DLS were used to study nanoscopic and mesoscopic dynamics to understand how the nanoscopic structure affects the nanoscopic molecular dynamics. NSE spectroscopy has been quite successful in exploring molecular motions in vesicles.⁶⁵⁻⁶⁷

2 Theory

2.1 Morphology

The 1D SANS scattering pattern for a unilamellar PEG-PDMS-PEG polymersome can be described by²³

$$I(Q, R, t, \Delta\rho) = \frac{d\Sigma}{d\Omega}(Q) = \frac{\phi[A(Q)]^2}{V(r_3) - V(R_c)} \quad (1)$$

Here ϕ is the block copolymer volume fraction. The scattering contribution from three different shells consisting of PEG, PDMS, and PEG are given by

$$A^2(Q) = A_1^2 + A_2^2 + A_3^2 + A_{12} + A_{23} + A_{13} \quad (2)$$

with $A_{12} = 2A_1A_2$, $A_{12} = 2A_2A_3$, and $A_{13} = 2A_1A_3$ are the cross terms for PEG-PDMS, PDMS-PEG, and the two outer PEG-PEG layers, respectively. Here $r_3 = R_p = R_c + 2t_{PEG} + t_{PDMS}$ is

the outer radius of the vesicle, with the radius of the core, R_c , the thickness of the PEG shells, t_{PEG} , and the thickness of the PDMS shell, t_{PDMS} . This model has been adapted for modified core-shell model used for vesicles.⁶⁸⁻⁷⁰ A modified core-shell model used for micelles has also been adapted based on our previous studies.^{71, 72} The 1-D SANS scattering pattern is given by:

$$I(Q) = \frac{d\Sigma}{d\Omega}(Q) = \frac{\phi}{V_m} [I_{core}(Q) + I_{corona}^b(Q) + I_{inter}(Q) + I_{blob}(Q)] \quad (3)$$

Here V_m and ϕ are the micelles' volume and volume fraction, respectively. The terms $I_{core}(Q)$ and $I_{corona}^b(Q)$ correspond to the scattering contribution from the micellar core and corona, respectively. The third contribution, $I_{inter}(Q)$, comes from the interference terms between the core and the corona and the blob scattering, $I_{blob}(Q)$, from the swollen corona is implemented following Svaneborg and Pedersen.⁷³

2.2 Dynamics

A simple approach to analyze the intermediate scattering function, $S(Q,t)$, as determined by NSE experiments, uses the Zilman-Granek (ZG) model that introduces the bending rigidity to describe the membrane dynamics⁷⁴

$$\frac{S(Q,t)}{S(Q)} = \exp \left[-(\Gamma_Q t)^{2/3} \right]. \quad (4)$$

The only free parameter is the Q -dependent decay rate, Γ_Q , from which we derive the intrinsic bending modulus, κ_η , by^{66, 75, 76}

$$\frac{\Gamma_Q}{Q^3} = 0.0069 \gamma \frac{k_B T}{\eta} \sqrt{\frac{k_B T}{\kappa_\eta}} \quad (5)$$

Here η is the viscosity, k_B the Boltzmann constant, T the temperature, and γ is a weak, monotonously increasing function of $\kappa_\eta/k_B T$.⁷⁴ In case of lipid bilayers usually $\kappa_\eta/k_B T \gg 1$, leading to $\gamma = 1$.^{65, 66, 74, 76, 77} Equation 5 can be derived from a modified ZG theory that includes intermonolayer friction. A detailed discussion is omitted here but can be found in the literature.^{66, 75, 76}

In addition, the contribution of the translational center of mass diffusion, D_t , of the liposomes needs to be included in the analysis of the dynamic structure factor, and we rewrite equation 1^{66, 78}

$$\frac{S(Q, t)}{S(Q)} = \exp(-D_t Q^2 t) \exp \left[-(\Gamma_q t)^{2/3} \right] \quad (6)$$

assuming ZG motion and center of mass diffusion are statistically independent. The separate measurement of D_t by DLS avoids additional free parameters. Alternative concepts may use a stretched exponent Kohlrausch-Williams-Watts (KWW) function coupled to the diffusion, D_t given by

$$\frac{S(Q, t)}{S(Q)} = \exp(-D_t Q^2 t) \exp \left[-\left(\frac{t}{\tau}\right)^\beta \right] \quad (7)$$

The KWW function is very popular in explaining the polymer dynamics in melts, solutions, and glassy materials.⁷⁹⁻⁸² This empirical approach has the advantage that it does not assume any particular concept and can provide information about the nature of the sub-diffusive behavior of the polymer chain exhibiting Zimm - or Rouse-type relaxation.

3 Experimental

Sample Preparation. The two amphiphilic triblock copolymers were synthesized via hydrosilylation between hydride-terminated PDMS blocks and allyloxy (poly(ethylene oxide)) methyl ether blocks, as described in our previous work.^{23, 83} The PEG₁₄-PDMS₁₅-PEG₁₄ and PEG₂₈-PDMS₁₅-PEG₂₈ polymers were dissolved in D₂O and subjected to sonication for 30 seconds using a probe sonicator. To obtain monodisperse unilamellar vesicles, the resulted solution for the PEG₁₄-PDMS₁₅-PEG₁₄ polymer was extruded through a 0.1 μm pore size polycarbonate membrane using a double-syringe mini-extruder (Avanti Polar Lipids, Alabaster, AL, Canada).

Dynamic Light Scattering (DLS) measurements were performed using a Malvern Zetasizer Nano ZS equipped with a He-Ne laser of wavelength $\lambda = 633$ nm at 30 mW laser power, at a scattering angle $\theta = 173^\circ$.

Cryogenic-transmission electron microscopy (cryo-TEM) images were recorded in the bright field setting on a Tecnai G2 F30 operated at 150 kV and a JEOL 1230 operated at 40 – 120 kV.

Small-angle neutron scattering (SANS) experiments were conducted at the NG 7 SANS instrument of the NIST Center for Neutron Research (NCNR) at the National Institute of Standards and Technology (NIST).⁸⁴ The sample-to-detector distances, d , were fixed to 1, 4, and 13 m at neutron wavelength, $\lambda = 6 \text{ \AA}$. Another configuration with lenses at $d = 15.3 \text{ m}$ and $\lambda = 8 \text{ \AA}$ was used to access low Q -values.⁸⁵ This combination covers a Q - range from ≈ 0.001 to $\approx 0.6 \text{ \AA}^{-1}$, where $Q = 4\pi \sin(\theta/2) / \lambda$, with the scattering angle, θ . A wavelength resolution of $\Delta\lambda/\lambda = 14\%$ was used. All data reduction into intensity, $I(Q)$, vs. momentum transfer, $Q = |\vec{Q}|$ was carried out following the standard procedures implemented in the NCNR macros for the Igor software package.⁸⁶ The intensity values were scaled into absolute units (cm^{-1}) using the direct beam. The solvents and the empty cell were measured separately as backgrounds.

Neutron spin echo spectroscopy (NSE) was conducted at SNS-NSE BL15 at the Spallation Neutron Source of the Oak Ridge National Laboratory, Oak Ridge, TN.⁸⁷ We used Hellma quartz cells with a 2 mm sample thickness. Measurements were conducted at an incident wavelength of 8 \AA . The BL15 Dr. Spine software package was used for data reduction.

4 Results and Discussion

Hereafter, we concentrate on two triblock copolymers based on poly(dimethyl siloxane) (PDMS) and poly(ethylene glycol) blocks, PEG₁₄-PDMS₁₅-PEG₁₄ and PEG₂₈-PDMS₁₅-PEG₂₈. The index indicates the number of repeating units in each block.

As illustrated in Figure 1, we have calculated the electric field autocorrelation function, $g_e^1(Q, t)$, which for identical interacting spheres gives the normalized dynamic structure factor, $S(Q, t)/S(Q)$. The data has been modeled using a simple diffusion model, $\exp(-D_t Q^2 t)$, to obtain the translational diffusion coefficient, D_t . The hydrodynamic radius, R_h , of each self-assembled structure was calculated using the Stokes-Einstein equation, $R_h = k_B T / (6\pi\eta_0 D_t)$, with the Boltzmann constant, k_B , the temperature, T , and the viscosity of the solvent (D_2O), $\eta_0 = 1.0945 \text{ cP}$.⁸⁸ D_2O has a lower background than H_2O in SANS and NSE experiments. Hence, we used D_2O also for DLS.

We obtain $R_h = 59.5 \pm 0.5$ nm for the PEG₁₄-PDMS₁₅-PEG₁₄ polymersome, with $D_t = (3.37 \pm 0.03) \times 10^{-12}$ m²s⁻¹. For PEG₂₈-PDMS₁₅-PEG₂₈ micelles, we obtain $R_h = 8.02 \pm 0.07$ nm, with $D_t = (24.9 \pm 0.2) \times 10^{-12}$ m²s⁻¹.

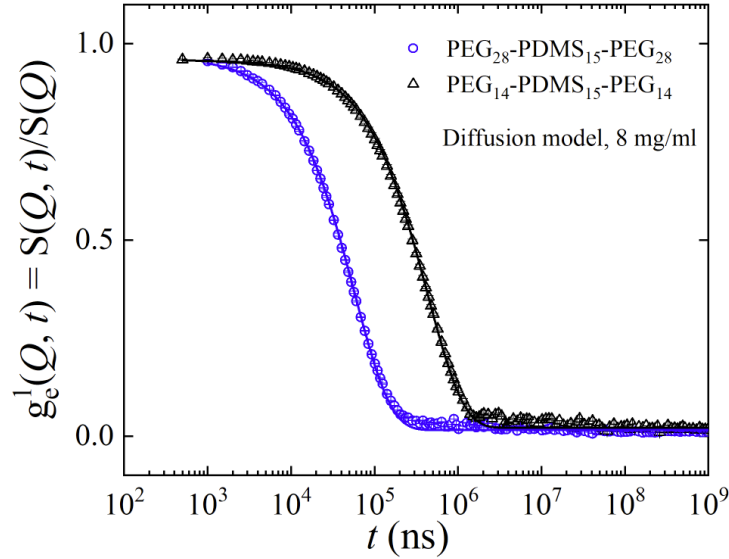


Figure 1. The electric field autocorrelation function, $g_e^1(Q, t)$, from DLS as a function of lag time for PEG₂₈-PDMS₁₅-PEG₂₈, and PEG₁₄-PDMS₁₅-PEG₁₄ tri-block copolymer samples at 8 mg/ml concentrations. The solid lines represent the fits using a simple diffusion model, as explained in the text.

Figure 2a illustrates the SANS scattering intensity normalized by their volume fraction, ϕ , for the PEG₂₈-PDMS₁₅-PEG₂₈ and PEG₁₄-PDMS₁₅-PEG₁₄ polymers. The results for PEG₁₄-PDMS₁₅-PEG₁₄ are modeled using a vesicle form factor, equation 1.^{69, 70} Our SANS analysis yields the total number of polymers per polymersome, $N_{agg} = 65954 \pm 128$, with the PEG and PDMS thickness of 0.6 ± 0.2 nm and 5 ± 0.8 nm, respectively. These values correspond to a PEG₁₄-PDMS₁₅-PEG₁₄ membrane thickness of 5.6 ± 1.0 nm. The corresponding outer perimeter radius $R_{SANS} = R_p = 59.2 \pm 2.0$ nm with a particle polydispersity of 30 ± 2 %, obtained from a log-normal size distribution.

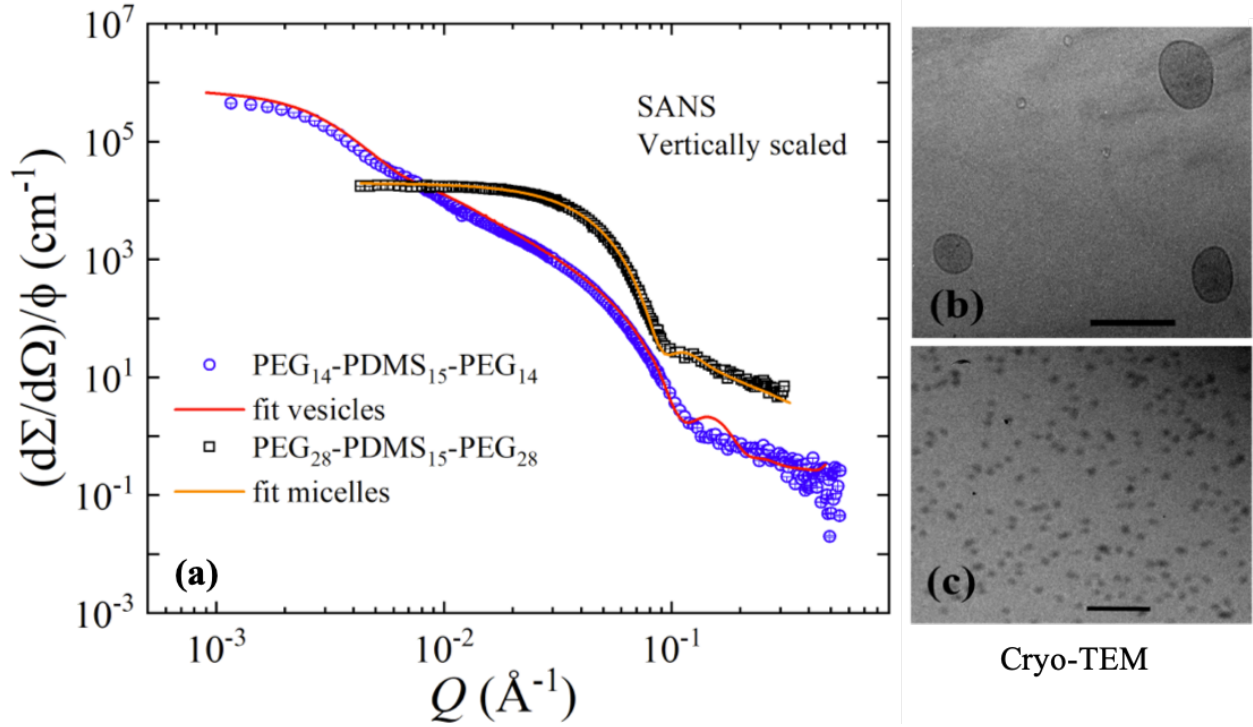


Figure 2. (a) SANS scattering intensity normalized by their volume fraction, ϕ , for PEG_{14} - $PDMS_{15}$ - PEG_{14} , and PEG_{28} - $PDMS_{15}$ - PEG_{28} tri-block copolymer samples at 8 mg/ml concentrations dispersed in D_2O . The solid lines represent the fits using a vesicle and a micelle model. Cryo-TEM images of self-assembled structures of (b) PEG_{14} - $PDMS_{15}$ - PEG_{14} and (c) PEG_{28} - $PDMS_{15}$ - PEG_{28} with scale bars representing 200 and 50 nm, respectively.

Instead, the data for the PEG_{28} - $PDMS_{15}$ - PEG_{28} polymer have been modeled using the micelle form factor, equation 3.^{71, 72} We obtain a micellar radius, $R_{SANS} = R_m = 5.1 \pm 0.7$ nm. The micellar core radius is given by $R_c = 3.4 \pm 0.1$ nm, where the standard deviation of a Gaussian distribution, $\sigma_G = 0.19 \pm 0.01$, has been used to define the corona-solvent interface of the micelle. The corresponding aggregation number, i.e., the number of polymers per micelles, $N_{agg} = 100 \pm 4$.

Figure 2b illustrates the cryo-TEM images of the PEG_{14} - $PDMS_{15}$ - PEG_{14} polymer that forms unilamellar polydisperse vesicles with the largest diameter of around 200 nm and the smallest diameter of around 88 nm. The average membrane thickness of the vesicles was 6 ± 1 nm. As illustrated in Figure 2c, PEG_{28} - $PDMS_{15}$ - PEG_{28} polymer self-assembled into micelles with an average diameter of 3.5 nm.

The macromolecular dynamics ultimately determine the structural stability. Hence, in our next step, we explore the dynamics of the PEG₁₄-PDMS₁₅-PEG₁₄ and PEG₂₈-PDMS₁₅-PEG₂₈ triblock copolymers.

Figure 3a illustrates the normalized dynamic structure factor, $S(Q, t)/S(Q)$, covering a Q -range from 0.035 to 0.094 Å⁻¹, measured by NSE for the vesicular sample (PEG₁₄-PDMS₁₅-PEG₁₄). The data can be modeled using the ZG (equation 5) and the KWW models (equation 7), as illustrated by the solid and dashed lines. The translational diffusion, D_t , from DLS, was kept as a fixed parameter. The corresponding stretched exponent obtained from the KWW fits using equation 7 was $\beta = 0.59 \pm 0.02$. This β value is very close to 0.66 (= 2/3), as predicted by Zilman and Granek. The calculated curves are very similar. Overall, the ZG equation describes the experimental results well and yields a membrane rigidity of $\kappa_\eta = 16 \pm 2 k_B T$, as obtained from Figure 4.

We also point to two famous models, Rouse dynamics ($\beta \approx 0.5$) of polymers in melts and Zimm-like motion ($\beta \approx 0.66$) for polymers in solution.^{79, 89} Recent studies on poly(styrene)-poly(butadiene) (PS-PB) block copolymer micelles suggested melt-like behavior of PB hydrophobic core in n-hexadecane and DMF.⁹⁰ This, along with our analysis, opens up the possibilities for a Zimm-Rouse-like motion exhibited by the triblock copolymer in a selective solvent.

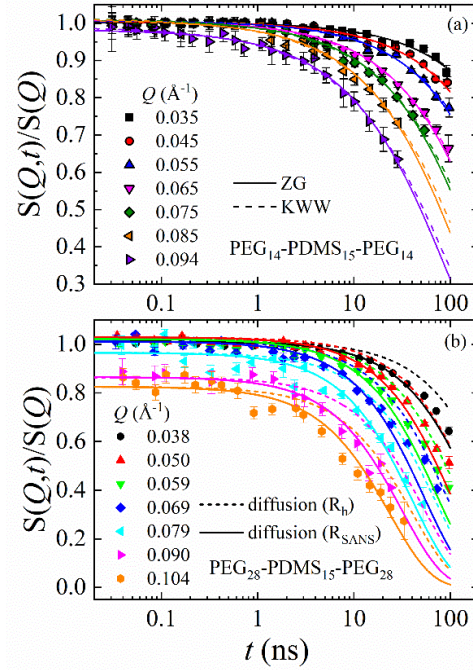


Figure 3. Dynamic structure factor, $S(Q,t)/S(Q)$, as a function of Fourier time, t , for different Q 's for PEG_{14} - $PDMS_{15}$ - PEG_{14} and PEG_{28} - $PDMS_{15}$ - PEG_{28} tri-block copolymer samples at 8 mg/ml concentrations dispersed in D_2O . The vesicle data in (a) is modeled using the ZG (equation 5) and KWW (equation 7) models, presented by the solid and the dashed lines, respectively. The micelle data in (b) is compared to the translational diffusion, $\exp(-D_t Q^2 t)$, of a rigid sphere. For illustration, the translational diffusion coefficient, D_t , has been calculated from the hydrodynamic radius, R_h , (dashed lines), and the micellar perimeter radius, R_m , (solid lines).

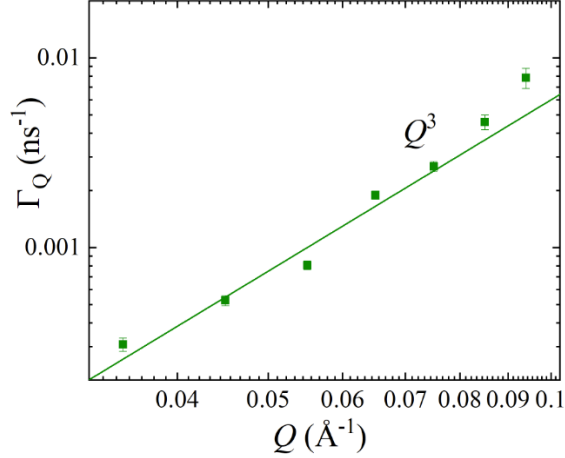


Figure 4. Zilman-Granek (ZG) parameter, Γ_Q , vs. momentum transfer, Q . The full line represents calculations with Equation 5.

Figure 3b illustrates the normalized dynamic structure factor, $S(Q, t)/S(Q)$, measured by NSE for the micellar sample (PEG₂₈-PDMS₁₅-PEG₂₈), covering a Q -range from 0.038 to 0.104 \AA^{-1} . The comparison of data modeling following the translational diffusion, described by the diffusion coefficient $D_t = k_B T / (6\pi\eta_0 R_{h/m})$ corresponding to hydrodynamic radius, R_h , from DLS and the micellar radius, R_m , from SANS has been performed. The good agreement of the model with the experimental results indicates that the micelles' observed dynamics structure factor $S(Q, t)/S(Q)$ of the micellar sample is governed by translational diffusion.

5 Conclusion

We investigated the molecular structure and dynamics of the two amphiphilic triblock copolymers, PEG₁₄-PDMS₁₅-PEG₁₄ and PEG₂₈-PDMS₁₅-PEG₂₈. Small-angle neutron scattering and cryo-transmission electron microscopy confirmed the formation of vesicles and micelles. Neutron spin echo spectroscopy experiments show substantially different results, with a vesicle that can be well described by Zilman-Granek and Zimm dynamics and a micelle well represented by the translational center of mass diffusion. Hence, there is a substantial difference between the two different assembled structures. The membrane rigidity of $\kappa_\eta = 16 \pm 2 k_B T$ (at ambient temperature) is the same magnitude as the value measured for many liposomes. For example, depending on temperature, pH, and buffer conditions, DOPC is 20 $k_B T$.^{34, 35} Instead, it is much bigger than values observed for microemulsion with polymeric surfactants, typically in the order of 1 $k_B T$.^{91, 92} Although different materials have similar membrane-thickness since the lipid and

polymer-based vesicles, the observed bending rigidity is closer to the liposome values. It has been observed that the membrane rigidity approximately varies quadratically with an increase in thickness.⁹³ Hence, it is likely that polymer-based systems allow a wide variety of bending elasticities, from the low values found at interfaces at microemulsions to values that match those of vesicles based on lipids. In understanding the dynamics, these unique polymersomes are established as a model macromolecule that can bridge the gap between self-assembled microemulsions and liposomes. This is a first step forward in the fundamental understanding of the structure-morphology-dynamics of such a hybrid-macromolecular system, and further investigations are essential to determine the concentration dependence and influence of the chemical composition.

6 Author Information

6.1 Corresponding Authors

*Email: Sudipta Gupta g.sudipta26@gmail.com

*Email: Rasangi Perera mpere4@lsuhsc.edu

*Email: Gerald J. Schneider gjschneider@lsu.edu

6.2 ORCID

Sudipta Gupta: 0000-0001-6642-3776

Rasangi Perera: 0000-0002-1394-4006

Laura Stingaciu: 0000-0003-2696-5233

Markus Bleuel: 0000-0003-3923-9505

Kunlun Hong: 0000-0002-2852-5111

Gerald J. Schneider: 0000-0002-5577-9328

7 Notes

The authors declare no competing financial interest.

8 Acknowledgment

The neutron scattering work is supported by the U.S. Department of Energy (DOE) under EPSCoR Grant No. DE-SC0012432 with additional support from the Louisiana Board of Regents. The Center for High-Resolution Neutron Scattering provided access to the neutron spin echo spectrometer and small-angle scattering instruments, a partnership between the National Institute of Standards and Technology and the National Science Foundation under Agreement No. DMR-

1508249. Research conducted at the Spallation Neutron Source (SNS) at Oak Ridge National Laboratory (ORNL) was sponsored by the Scientific User Facilities Division, Office of Basic Energy Sciences, U.S. DOE. The polymer synthesis and characterization of this research was conducted at the Center for Nanophase Materials Sciences (CNMS), which is a DOE Office of Science User Facility. The Center for High-Resolution Neutron Scattering provided access to the NG7 SANS instrument, a partnership between the National Institute of Standards and Technology and the National Science Foundation under Agreement No. DMR-201079. We want to thank Jeff Krzywon for NG7 beamline support. We want to thank Rafael Cueto (LSU) for supporting DLS experiments and Jibao He (Tulane University) for his support in Cryo-TEM imaging.

9 References

- (1) Wang, X.; He, C.; Yang, Q.; Tan, L.; Liu, B.; Zhu, Z.; Gong, B.; Shen, Y. M. Dynamic covalent linked triblock copolymer micelles for glutathione-mediated intracellular drug delivery. *Mater Sci Eng C Mater Biol Appl* **2017**, *77*, 34-44. DOI: 10.1016/j.msec.2017.03.240.
- (2) Monzen, M.; Kawakatsu, T.; Doi, M.; Hasegawa, R. Micelle formation in triblock copolymer solutions. *Computational and Theoretical Polymer Science* **2000**, *10* (3), 275-280. DOI: [https://doi.org/10.1016/S1089-3156\(99\)00052-5](https://doi.org/10.1016/S1089-3156(99)00052-5).
- (3) Schillen, K.; Brown, W.; Johnsen, R. M. Micellar Sphere-to-Rod Transition in an Aqueous Triblock Copolymer System. A Dynamic Light Scattering Study of Translational and Rotational Diffusion. *Macromolecules* **1994**, *27* (17), 4825-4832. DOI: 10.1021/ma00095a025.
- (4) Wang, X.; Guerin, G.; Wang, H.; Wang, Y.; Manners, I.; Winnik, M. A. Cylindrical Block Copolymer Micelles and Co-Micelles of Controlled Length and Architecture. *Science (New York, N.Y.)* **2007**, *317* (5838), 644-647. (accessed 2020/03/27/).JSTOR.
- (5) Nardin, C.; Hirt, T.; Leukel, J.; Meier, W. Nanoreactors based on (polymerized) ABA-triblock copolymer vesicles. *Langmuir* **2000**, *16* (3), 1035-1041. DOI: 10.1021/la990951u.
- (6) Mable, C. J.; Fielding, L. A.; Derry, M. J.; Mykhaylyk, O. O.; Chambon, P.; Armes, S. P. Synthesis and pH-responsive dissociation of framboidal ABC triblock copolymer vesicles in aqueous solution. *Chemical Science* **2018**, *9* (6), 1454-1463, 10.1039/C7SC04788F. DOI: 10.1039/C7SC04788F.
- (7) Song, Y.; Xie, T.; Jiang, R.; Wang, Z.; Yin, Y.; Li, B.; Shi, A. C. Effect of Chain Architecture on Self-Assembled Aggregates from Cyclic AB Diblock and Linear ABA Triblock Copolymers in Solution. *Langmuir* **2018**, *34* (13), 4013-4023. DOI: 10.1021/acs.langmuir.8b00630.

- (8) Du, J.; O'Reilly, R. K. Advances and challenges in smart and functional polymer vesicles. *Soft Matter* **2009**, *5* (19), 3544-3561, 10.1039/B905635A. DOI: 10.1039/B905635A.
- (9) Palanisamy, A.; Guo, Q. Large compound vesicles from amphiphilic block copolymer/rigid-rod conjugated polymer complexes. *J Phys Chem B* **2014**, *118* (44), 12796-12803. DOI: 10.1021/jp508352a.
- (10) Liu, F.; Kozlovskaya, V.; Medipelli, S.; Xue, B.; Ahmad, F.; Saeed, M.; Cropek, D.; Kharlampieva, E. Temperature-Sensitive Polymersomes for Controlled Delivery of Anticancer Drugs. *Chemistry of Materials* **2015**, *27* (23), 7945-7956. DOI: 10.1021/acs.chemmater.5b03048.
- (11) Kamat, N. P.; Katz, J. S.; Hammer, D. A. Engineering Polymersome Protocells. *J Phys Chem Lett* **2011**, *2* (13), 1612-1623. DOI: 10.1021/jz200640x PubMed.
- (12) Broz, P.; Driamov, S.; Ziegler, J.; Ben-Haim, N.; Marsch, S.; Meier, W.; Hunziker, P. Toward Intelligent Nanosize Bioreactors: A pH-Switchable, Channel-Equipped, Functional Polymer Nanocontainer. *Nano Letters* **2006**, *6* (10), 2349-2353. DOI: 10.1021/nl0619305.
- (13) Iatrou, H.; Frielinghaus, H.; Hanski, S.; Ferderigos, N.; Ruokolainen, J.; Ikkala, O.; Richter, D.; Mays, J.; Hadjichristidis, N. Architecturally Induced Multiresponsive Vesicles from Well-Defined Polypeptides. Formation of Gene Vehicles. *Biomacromolecules* **2007**, *8* (7), 2173-2181. DOI: 10.1021/bm070360f.
- (14) Ghezzi, M.; Pescina, S.; Padula, C.; Santi, P.; Del Favero, E.; Cantù, L.; Nicoli, S. Polymeric micelles in drug delivery: An insight of the techniques for their characterization and assessment in biorelevant conditions. *Journal of Controlled Release* **2021**, *332*, 312-336. DOI: <https://doi.org/10.1016/j.jconrel.2021.02.031>.
- (15) Geng, Y.; Dalhaimer, P.; Cai, S.; Tsai, R.; Tewari, M.; Minko, T.; Discher, D. E. Shape effects of filaments versus spherical particles in flow and drug delivery. *Nature Nanotechnology* **2007**, *2* (4), 249-255. DOI: 10.1038/nnano.2007.70.
- (16) Kim, Y.; Dalhaimer, P.; Christian, D. A.; Discher, D. E. Polymeric worm micelles as nano-carriers for drug delivery. *Nanotechnology* **2005**, *16* (7), S484-S491. DOI: 10.1088/0957-4484/16/7/024.
- (17) Seifert, U.; Berndl, K.; Lipowsky, R. Shape transformations of vesicles: Phase diagram for spontaneous- curvature and bilayer-coupling models. *Physical Review A* **1991**, *44* (2), 1182-1202. DOI: 10.1103/PhysRevA.44.1182.

- (18) Goren, M.; Lennox, R. B. Nanoscale Polypyrrole Patterns Using Block Copolymer Surface Micelles as Templates. *Nano Letters* **2001**, *1* (12), 735-738. DOI: 10.1021/nl015630t.
- (19) Kozlov, M. Y.; Melik-Nubarov, N. S.; Batrakova, E. V.; Kabanov, A. V. Relationship between Pluronic Block Copolymer Structure, Critical Micellization Concentration and Partitioning Coefficients of Low Molecular Mass Solutes. *Macromolecules* **2000**, *33* (9), 3305-3313. DOI: 10.1021/ma991634x.
- (20) Riess, G. Micellization of block copolymers. *Progress in Polymer Science* **2003**, *28* (7), 1107-1170. DOI: 10.1016/s0079-6700(03)00015-7.
- (21) J. Prasad Rao, K. E. G. Polymer nanoparticles: Preparation techniques and size-control parameters. *Progress in Polymer Science* **2011**, *36* (7), 887-913. DOI: 10.1016/j.progpolymsci.2011.01.001.
- (22) Matoori, S.; Leroux, J.-C. Twenty-five years of polymersomes: lost in translation? *Materials Horizons* **2020**, *7* (5), 1297-1309. DOI: 10.1039/c9mh01669d.
- (23) Perera, R. M.; Gupta, S.; Li, T.; Bleuel, M.; Hong, K.; Schneider, G. J. Influence of NaCl on shape deformation of polymersomes. *Soft Matter* **2021**, *17* (16), 4452-4463, 10.1039/D0SM02271C. DOI: 10.1039/d0sm02271c.
- (24) Kozlovskaya, V.; Liu, F.; Yang, Y.; Ingle, K.; Qian, S.; Halade, G. V.; Urban, V. S.; Kharlampieva, E. Temperature-Responsive Polymersomes of Poly(3-methyl-N-vinylcaprolactam)-block-poly(N-vinylpyrrolidone) To Decrease Doxorubicin-Induced Cardiotoxicity. *Biomacromolecules* **2019**, *20* (10), 3989-4000. DOI: 10.1021/acs.biomac.9b01026.
- (25) Men, Y.; Li, W.; Lebleu, C.; Sun, J.; Wilson, D. A. Tailoring Polymersome Shape Using the Hofmeister Effect. *Biomacromolecules* **2020**, *21* (1), 89-94. DOI: 10.1021/acs.biomac.9b00924.
- (26) Pearson, R. T.; Warren, N. J.; Lewis, A. L.; Armes, S. P.; Battaglia, G. Effect of pH and Temperature on PMPC-PDPA Copolymer Self-Assembly. *Macromolecules* **2013**, *46* (4), 1400-1407. DOI: 10.1021/ma302228m.
- (27) Chécot, F.; Brûlet, A.; Oberdisse, J.; Gnanou, Y.; Mondain-Monval, O.; Lecommandoux, S. Structure of Polypeptide-Based Diblock Copolymers in Solution: Stimuli-Responsive Vesicles and Micelles. *Langmuir* **2005**, *21* (10), 4308-4315. DOI: 10.1021/la0468500.
- (28) Fauquignon, M.; Ibarboure, E.; Carlotti, S.; Brulet, A.; Schmutz, M.; Le Meins, J. F. Large and Giant Unilamellar Vesicle(s) Obtained by Self-Assembly of Poly(dimethylsiloxane)-b-

poly(ethylene oxide) Diblock Copolymers, Membrane Properties and Preliminary Investigation of their Ability to Form Hybrid Polymer/Lipid Vesicles. *Polymers (Basel)* **2019**, *11* (12). DOI: 10.3390/polym11122013.

(29) Fetsch, C.; Gaitzsch, J.; Messenger, L.; Battaglia, G.; Luxenhofer, R. Self-Assembly of Amphiphilic Block Copolypeptoids - Micelles, Worms and Polymersomes. *Sci Rep* **2016**, *6*, 33491. DOI: 10.1038/srep33491.

(30) Bermudez, H.; Brannan, A. K.; Hammer, D. A.; Bates, F. S.; Discher, D. E. Molecular Weight Dependence of Polymersome Membrane Structure, Elasticity, and Stability. *Macromolecules* **2002**, *35* (21), 8203-8208. DOI: 10.1021/ma020669l.

(31) Pencer, J.; White, G. F.; Hallett, F. R. Osmotically Induced Shape Changes of Large Unilamellar Vesicles Measured by Dynamic Light Scattering. *Biophysical Journal* **2001**, *81* (5), 2716-2728. DOI: [https://doi.org/10.1016/S0006-3495\(01\)75914-0](https://doi.org/10.1016/S0006-3495(01)75914-0).

(32) Salva, R.; Le Meins, J.-F.; Sandre, O.; Brûlet, A.; Schmutz, M.; Guenoun, P.; Lecommandoux, S. Polymersome Shape Transformation at the Nanoscale. *ACS Nano* **2013**, *7* (10), 9298-9311. DOI: 10.1021/nn4039589.

(33) Yang, Y.; Alford, A.; Kozlovskaya, V.; Zhao, S.; Joshi, H.; Kim, E.; Qian, S.; Urban, V.; Cropek, D.; Aksimentiev, A.; et al. Effect of temperature and hydrophilic ratio on the structure of poly(N-vinylcaprolactam)-block-poly(dimethylsiloxane)-block-poly(N-vinylcaprolactam) polymersomes. *ACS Appl Polym Mater* **2019**, *1* (4), 722-736. DOI: 10.1021/acsapm.8b00259.

(34) Gupta, S.; De Mel, J. U.; Schneider, G. J. Dynamics of liposomes in the fluid phase. *Current Opinion in Colloid & Interface Science* **2019**, *42*, 121-136. DOI: 10.1016/j.cocis.2019.05.003.

(35) Gupta, S.; De Mel, J. U.; Perera, R. M.; Zolnierczuk, P.; Bleuel, M.; Faraone, A.; Schneider, G. J. Dynamics of Phospholipid Membranes beyond Thermal Undulations. *J Phys Chem Lett* **2018**, *9* (11), 2956-2960. DOI: 10.1021/acs.jpcclett.8b01008.

(36) De Mel, J. U.; Gupta, S.; Perera, R. M.; Ngo, L.; Zolnierczuk, P.; Bleuel, M.; Pingali, S. V.; Schneider, G. J. Influence of External NaCl Salt on Membrane Rigidity of Neutral DOPC Vesicles. *Langmuir* **2020**, *36* (32), 9356-9367. DOI: 10.1021/acs.langmuir.0c01004.

(37) Gupta, S.; Schneider, G. J. Modeling the dynamics of phospholipids in the fluid phase of liposomes. *Soft Matter* **2020**, *16* (13), 3245-3256. DOI: 10.1039/c9sm02111f.

- (38) Tekpli, X.; A. Holme, J.; Sergent, O.; Lagadic-Gossmann, D. Importance of Plasma Membrane Dynamics in Chemical-Induced Carcinogenesis. *Recent Patents on Anti-Cancer Drug Discovery* **2011**, *6* (3), 347-353. DOI: 10.2174/157489211796957784.
- (39) Liu, J.; Qi, S.; Groves, J. T.; Chakraborty, A. K. Phase Segregation on Different Length Scales in a Model Cell Membrane System. *The Journal of Physical Chemistry B* **2005**, *109* (42), 19960-19969. DOI: 10.1021/jp053562j.
- (40) Cornell, C. E.; Skinkle, A. D.; He, S.; Levental, I.; Levental, K. R.; Keller, S. L. Tuning Length Scales of Small Domains in Cell-Derived Membranes and Synthetic Model Membranes. *Biophysical Journal* **2018**, *115* (4), 690-701. DOI: <https://doi.org/10.1016/j.bpj.2018.06.027>.
- (41) Fan, L.-t.; Singh, S. K. *Controlled release: A quantitative treatment*; Springer Science & Business Media, 2012.
- (42) Rideau, E.; Dimova, R.; Schwille, P.; Wurm, F. R.; Landfester, K. Liposomes and polymersomes: a comparative review towards cell mimicking. *Chemical Society Reviews* **2018**, *47* (23), 8572-8610, 10.1039/C8CS00162F. DOI: 10.1039/C8CS00162F.
- (43) Yorulmaz Avsar, S.; Kyropoulou, M.; Di Leone, S.; Schoenenberger, C. A.; Meier, W. P.; Palivan, C. G. Biomolecules Turn Self-Assembling Amphiphilic Block Co-polymer Platforms Into Biomimetic Interfaces. *Front Chem* **2018**, *6*, 645. DOI: 10.3389/fchem.2018.00645.
- (44) Sanders, T. J. Suitability of Biodegradable Polymersomes as Radionuclide Carriers. Delft University of Technology, 2014.
- (45) Wong, C. K.; Stenzel, M. H.; Thordarson, P. Non-spherical polymersomes: formation and characterization. *Chem Soc Rev* **2019**, *48* (15), 4019-4035. DOI: 10.1039/c8cs00856f.
- (46) Hutanu, D. Recent Applications of Polyethylene Glycols (PEGs) and PEG Derivatives. *Modern Chemistry & Applications* **2014**, *02* (02). DOI: 10.4172/2329-6798.1000132.
- (47) Maitz, M. F. Applications of synthetic polymers in clinical medicine. *Biosurface and Biotribology* **2015**, *1* (3), 161-176. DOI: <https://doi.org/10.1016/j.bsbt.2015.08.002>.
- (48) Zalipsky, S., Harris, J.M., Introduction to Chemistry and Biological Applications of Poly (ethylene glycol). In *ACS Symposium Series*, Washington, DC, 1997; J. Milton Harris, S. Z., Ed.; American Chemical Society: Vol. 680. DOI: 10.1021/bk-1997-0680.
- (49) Li, N.; Echeverria, M.; Moya, S.; Ruiz, J.; Astruc, D. "Click" synthesis of nona-PEG-branched triazole dendrimers and stabilization of gold nanoparticles that efficiently catalyze p-nitrophenol reduction. *Inorg Chem* **2014**, *53* (13), 6954-6961. DOI: 10.1021/ic500861f.

- (50) Chan, R. T. H.; Marçal, H.; Russell, R. A.; Holden, P. J.; Foster, L. J. R. Application of Polyethylene Glycol to Promote Cellular Biocompatibility of Polyhydroxybutyrate Films. *International Journal of Polymer Science* **2011**, *2011*, 1-9. DOI: 10.1155/2011/473045.
- (51) Huang, Q.; Li, D.; Kang, A.; An, W.; Fan, B.; Ma, X.; Ma, G.; Su, Z.; Hu, T. PEG as a spacer arm markedly increases the immunogenicity of meningococcal group Y polysaccharide conjugate vaccine. *Journal of Controlled Release* **2013**, *172* (1), 382-389, Article. DOI: 10.1016/j.jconrel.2013.03.008 From EBSCOhost edselp.
- (52) Badi, N. Non-linear PEG-based thermoresponsive polymer systems. *Progress in Polymer Science* **2017**, *66*, 54-79. DOI: 10.1016/j.progpolymsci.2016.12.006.
- (53) Liu, X. Y.; Nothias, J. M.; Scavone, A.; Garfinkel, M.; Millis, J. M. Biocompatibility investigation of polyethylene glycol and alginate-poly-L-lysine for islet encapsulation. *ASAIO journal (American Society for Artificial Internal Organs : 1992)* **2010**, *56* (3), 241-245. DOI: 10.1097/MAT.0b013e3181d7b8e3 From NLM.
- (54) Ionescu, M.; Winton, B.; Wexler, D.; Siegele, R.; Deslantes, A.; Stelcer, E.; Atanacio, A.; Cohen, D. D. Enhanced biocompatibility of PDMS (polydimethylsiloxane) polymer films by ion irradiation. *Nuclear Instruments and Methods in Physics Research Section B: Beam Interactions with Materials and Atoms* **2012**, *273*, 161-163. DOI: 10.1016/j.nimb.2011.07.065.
- (55) Stevens, C.; Powell, D. E.; Mäkelä, P.; Karman, C. Fate and Effects of Polydimethylsiloxane (PDMS) in Marine Environments. *Marine Pollution Bulletin* **2001**, *42* (7), 536-543. DOI: [https://doi.org/10.1016/S0025-326X\(00\)00229-0](https://doi.org/10.1016/S0025-326X(00)00229-0).
- (56) Feng, J.-T.; Zhao, Y.-P. Influence of different amount of Au on the wetting behavior of PDMS membrane. *Biomedical Microdevices* **2008**, *10* (1), 65-72. DOI: 10.1007/s10544-007-9110-2.
- (57) Subramaniam, A. S., Swaminathan. Chapter 18 - Biomedical Applications of Nondegradable Polymers. In *Natural and Synthetic Biomedical Polymers*, Kumbar, S. G., Laurencin, C. T., Deng, M. Eds.; Elsevier, 2014; pp 301-308.
- (58) Helfrich, W. Size distributions of vesicles: the role of the effective rigidity of membranes. *J. Phys. France* **1986**, *47* (2), 321-329. DOI: 10.1051 / jphys: 01986004702032100.
- (59) Dimova, R. Recent developments in the field of bending rigidity measurements on membranes. *Advances in Colloid and Interface Science* **2014**, *208*, 225-234. DOI: <https://doi.org/10.1016/j.cis.2014.03.003>.

- (60) Lindahl, E.; Edholm, O. Mesoscopic Undulations and Thickness Fluctuations in Lipid Bilayers from Molecular Dynamics Simulations. *Biophysical Journal* **2000**, *79* (1), 426-433. DOI: [https://doi.org/10.1016/S0006-3495\(00\)76304-1](https://doi.org/10.1016/S0006-3495(00)76304-1).
- (61) Imparato, A.; Shillcock, J. C.; Lipowsky, R. Shape fluctuations and elastic properties of two-component bilayer membranes. *Europhysics Letters (EPL)* **2005**, *69* (4), 650-656. DOI: 10.1209/epl/i2004-10382-3.
- (62) Arriaga, L. R.; López-Montero, I.; Monroy, F.; Orts-Gil, G.; Farago, B.; Hellweg, T. Stiffening Effect of Cholesterol on Disordered Lipid Phases: A Combined Neutron Spin Echo + Dynamic Light Scattering Analysis of the Bending Elasticity of Large Unilamellar Vesicles. *Biophysical Journal* **2009**, *96* (9), 3629-3637. DOI: <https://doi.org/10.1016/j.bpj.2009.01.045>.
- (63) Arriaga, L. R.; López-Montero, I.; Orts-Gil, G.; Farago, B.; Hellweg, T.; Monroy, F. Fluctuation dynamics of spherical vesicles: Frustration of regular bulk dissipation into subdiffusive relaxation. *Physical Review E* **2009**, *80* (3), 031908. DOI: 10.1103/PhysRevE.80.031908.
- (64) Yi, Z.; Bossev, D. Bending Elasticity of Bio-Membranes Studied by Neutron Spin-Echo. **2007**.
- (65) Woodka, A. C.; Butler, P. D.; Porcar, L.; Farago, B.; Nagao, M. Lipid bilayers and membrane dynamics: insight into thickness fluctuations. *Phys Rev Lett* **2012**, *109* (5), 058102. DOI: 10.1103/PhysRevLett.109.058102.
- (66) Hoffmann, I.; Michel, R.; Sharp, M.; Holderer, O.; Appavou, M. S.; Polzer, F.; Farago, B.; Gradzielski, M. Softening of phospholipid membranes by the adhesion of silica nanoparticles - as seen by neutron spin-echo (NSE). *Nanoscale* **2014**, *6* (12), 6945-6952. DOI: 10.1039/c4nr00774c.
- (67) Nickels, J. D.; Cheng, X.; Mostofian, B.; Stanley, C.; Lindner, B.; Heberle, F. A.; Perticaroli, S.; Feygenson, M.; Egami, T.; Standaert, R. F.; et al. Mechanical Properties of Nanoscopic Lipid Domains. *J Am Chem Soc* **2015**, *137* (50), 15772-15780. DOI: 10.1021/jacs.5b08894.
- (68) De Mel, J. U.; Gupta, S.; Willner, L.; Allgaier, J.; Stingaciu, L. R.; Bleuel, M.; Schneider, G. J. Manipulating Phospholipid Vesicles at the Nanoscale: A Transformation from Unilamellar to Multilamellar by an n-Alkyl-poly(ethylene oxide). *Langmuir* **2021**, *37* (7), 2362-2375. DOI: 10.1021/acs.langmuir.0c03302.
- (69) De Mel, J. U.; Gupta, S.; Perera, R. M.; Ngo, L. T.; Zolnierczuk, P.; Bleuel, M.; Pingali, S. V.; Schneider, G. J. Influence of external NaCl salt on membrane rigidity of neutral DOPC vesicles. *Langmuir* **2020**, *36*, 9356-9367. DOI: 10.1021/acs.langmuir.0c01004.

- (70) Gupta, S.; De Mel, J. U.; Perera, R. M.; Zolnierczuk, P.; Bleuel, M.; Faraone, A.; Schneider, G. J. Dynamics of Phospholipid Membranes beyond Thermal Undulations. *J Phys Chem Lett* **2018**, *9*, 2956-2960. DOI: 10.1021/acs.jpcclett.8b01008.
- (71) Sternhagen, G. L.; Gupta, S.; Zhang, Y.; John, V.; Schneider, G. J.; Zhang, D. Solution Self-Assemblies of Sequence-Defined Ionic Peptoid Block Copolymers. *Journal of American Chemical Society* **2018**, *140* (11), 4100-4109. DOI: 10.1021/jacs.8b00461.
- (72) Gupta, S.; Camargo, M.; Stellbrink, J.; Allgaier, J.; Radulescu, A.; Lindner, P.; Zaccarelli, E.; Likos, C. N.; Richter, D. Dynamic phase diagram of soft nanocolloids. *Nanoscale* **2015**, *7* (33), 13924-13934. DOI: 10.1039/c5nr03702f.
- (73) Pedersen, J. S.; Svaneborg, C.; Almdal, K.; Hamley, I. W.; Young, R. N. A Small-Angle Neutron and X-ray Contrast Variation Scattering Study of the Structure of Block Copolymer Micelles: Corona Shape and Excluded Volume Interactions. *Macromolecules* **2003**, *36* (2), 416-433. DOI: 10.1021/ma0204913.
- (74) Zilman, A. G.; Granek, R. Undulations and Dynamic Structure Factor of Membranes. *Phys Rev Lett* **1996**, *77* (23), 4788-4791. DOI: 10.1103/PhysRevLett.77.4788 From NLM Publisher.
- (75) Watson, M. C.; Brown, F. L. Interpreting membrane scattering experiments at the mesoscale: the contribution of dissipation within the bilayer. *Biophys J* **2010**, *98* (6), L9-L11. DOI: 10.1016/j.bpj.2009.11.026.
- (76) Nagao, M.; Kelley, E. G.; Ashkar, R.; Bradbury, R.; Butler, P. D. Probing Elastic and Viscous Properties of Phospholipid Bilayers Using Neutron Spin Echo Spectroscopy. *J Phys Chem Lett* **2017**, 4679-4684. DOI: 10.1021/acs.jpcclett.7b01830.
- (77) Takeda, T.; Kawabata, Y.; Seto, H.; Komura, S.; Ghosh, S. K.; Nagao, M.; Okuhara, D. Neutron spin-echo investigations of membrane undulations in complex fluids involving amphiphiles. *Journal of Physics and Chemistry of Solids* **1999**, *60* (8-9), 1375-1377. DOI: 10.1016/s0022-3697(99)00122-5.
- (78) Mell, M.; Moleiro, L. H.; Hertle, Y.; Fouquet, P.; Schweins, R.; Lopez-Montero, I.; Hellweg, T.; Monroy, F. Bending stiffness of biological membranes: what can be measured by neutron spin echo? *Eur Phys J E Soft Matter* **2013**, *36* (7), 75. DOI: 10.1140/epje/i2013-13075-2.
- (79) Richter, D.; Monkenbusch, M.; Arbe, A.; Colmenero, J. Neutron Spin Echo in Polymer Systems. *Adv Polym Sci* **2005**, *174*, 1 - 221. DOI: 10.1007/b106578.

- (80) Gupta, S.; Arend, N.; Lunkenheimer, P.; Loidl, A.; Stingaciu, L.; Jalarvo, N.; Mamontov, E.; Ohl, M. Excess wing in glass-forming glycerol and LiCl-glycerol mixtures detected by neutron scattering. *Eur Phys J E Soft Matter* **2015**, *38* (1), 1. DOI: 10.1140/epje/i2015-15001-0.
- (81) Gupta, S.; Fischer, J. K. H.; Lunkenheimer, P.; Loidl, A.; Novak, E.; Jalarvo, N.; Ohl, M. Effect of adding nanometre-sized heterogeneities on the structural dynamics and the excess wing of a molecular glass former. *Scientific Reports* **2016**, *6*, 35034. DOI: 10.1038/srep35034.
- (82) Gupta, S.; Mamontov, E.; Jalarvo, N.; Stingaciu, L.; Ohl, M. Characteristic length scales of the secondary relaxations in glass-forming glycerol. *Eur Phys J E Soft Matter* **2016**, *39* (3), 40. DOI: 10.1140/epje/i2016-16040-7.
- (83) Perera, R. M.; Gupta, S.; Li, T.; Van Leeuwen, C. J.; Bleuel, M.; Hong, K.; Schneider, G. J. Nanoscale Lipid/Polymer Hybrid Vesicles: Effects of Triblock Copolymer Composition and Hydrophilic Weight Fraction. *ACS Applied Polymer Materials* **2022**, *4* (12), 8858-8868. DOI: 10.1021/acsapm.2c01272.
- (84) Glinka, C. J.; Barker, J. G.; Hammouda, B.; Krueger, S.; Moyer, J. J.; Orts, W. J. The 30 m Small-Angle Neutron Scattering Instruments at the National Institute of Standards and Technology. *Journal of Applied Crystallography* **1998**, *31* (3), 430-445. DOI: 10.1107/s0021889897017020.
- (85) Choi, S. M.; Barker, J. G.; Glinka, C. J.; Cheng, Y. T.; Gammel, P. L. Focusing cold neutrons with multiple biconcave lenses for small-angle neutron scattering. *Journal of Applied Crystallography* **2000**, *33* (3), 793-796. DOI: 10.1107/s0021889800099799.
- (86) Kline, S. R. Reduction and analysis of SANS and USANS data using IGOR Pro. *Journal of Applied Crystallography* **2006**, *39* (6), 895-900. DOI: 10.1107/s0021889806035059.
- (87) Ohl, M.; Monkenbusch, M.; Arend, N.; Kozielowski, T.; Vehres, G.; Tiemann, C.; Butzek, M.; Soltner, H.; Giesen, U.; Achten, R.; et al. The spin-echo spectrometer at the Spallation Neutron Source (SNS). *Nuclear Instruments and Methods in Physics Research Section A: Accelerators, Spectrometers, Detectors and Associated Equipment* **2012**, *696*, 85-99. DOI: 10.1016/j.nima.2012.08.059.
- (88) Millero, F. J.; Dexter, R.; Hoff, E. Density and viscosity of deuterium oxide solutions from 5-70.deg. *Journal of Chemical & Engineering Data* **1971**, *16* (1), 85-87. DOI: 10.1021/jc60048a006.

- (89) Ewen, B.; Richter, D. Neutron spin echo investigations on the segmental dynamics of polymers in melts, networks and solutions. *Adv Polym Sci* **1997**, *134*, 1-129. DOI: 10.1007/3-540-68449-2_1.
- (90) Lund, R.; Willner, L.; Stellbrink, J.; Lindner, P.; Richter, D. Logarithmic chain-exchange kinetics of diblock copolymer micelles. *Phys Rev Lett* **2006**, *96* (6), 068302. DOI: 10.1103/PhysRevLett.96.068302.
- (91) Monkenbusch, M.; Holderer, O.; Frielinghaus, H.; Byelov, D.; Allgaier, J.; Richter, D. Bending moduli of microemulsions; comparison of results from small angle neutron scattering and neutron spin-echo spectroscopy. *Journal of Physics: Condensed Matter* **2005**, *17* (31), S2903. DOI: 10.1088/0953-8984/17/31/017.
- (92) Sharma, V.; Hayes, D.; Gupta, S.; Urban, V.; O'Neill, H.; Pingali, S.; Ohl, M.; Mamontov, E. Incorporation of melittin enhances interfacial fluidity of bicontinuous microemulsions. *The Journal of Physical Chemistry C* **2019**, *123* (17), 11197-11206. DOI: 10.1021/acs.jpcc.9b00103.
- (93) Nagle, J. F. Introductory lecture: basic quantities in model biomembranes. *Faraday Discuss* **2013**, *161*, 11-29; discussion 113-150. DOI: 10.1039/c2fd20121f.